cis-Bis(bipyridine)ruthenium Imidazole Derivatives: A Spectroscopic, Kinetic, and Structural Study

K. Bal Reddy, Myung-ok P. Cho, James F. Wishart,† Thomas J. Emge, and Stephan S. Isied*

Department of Chemistry, Rutgers, The State University of New Jersey, Piscataway, New Jersey 08855-0939

Received November 9, 1995[⊗]

The ruthenium bis(bipyridine) complexes *cis*-$[Ru(bpy)_2Im(OH_2)]^{2+}$, *cis*-$[Ru(bpy)_2(Im)_2]^{2+}$, *cis*-$[Ru(bpy)_2(N\text{-}Im)_2]^{2+}$, *cis*-$[Ru(dmbpy)_2Im(OH_2)]^{2+}$, *cis*-$[Ru(dmbpy)_2(N\text{-}Im)(OH_2)]^{2+}$(bpy = 2,2′-bipyridine, dmbpy = 4,4′-dimethyl-2,2′-bipyridine, Im = imidazole, N-Im = *N*-methylimidazole), have been synthesized under ambient conditions in aqueous solution (pH 7). Their electrochemical and spectroscopic properties, absorption, emission, and lifetimes were determined and compared. The substitution kinetics of the *cis*-$[Ru(bpy)_2Im(OH_2)]^{2+}$ complexes show slower rates and have lower affinities for imidazole ligands than the corresponding *cis*-$[Ru(NH_3)_4Im(OH_2)]^{2+}$ complexes. The crystal structures of the monoclinic *cis*-$[Ru(bpy)_2(Im)_2](BF_4)_2$, space group = $P2_1/a$, $Z = 4$, $a = 11.344(1)$ Å, $b = 17.499(3)$ Å, $c = 15.114(3)$ Å, and $\beta = 100.17(1)°$, and triclinic *cis*-$[Ru(bpy)_2(N\text{-}Im)(H_2O)](CF_3COO)_2 \cdot H_2O$, space group = $P\bar{1}$, $Z = 2$, $a = 10.432(4)$ Å, $b = 11.995(3)$ Å, $c = 13.912(5)$ Å, $\alpha = 87.03(3)°$, $\beta = 70.28(3)°$, and $\gamma = 71.57(2)°$, complexes show that these molecules crystallize as complexes of octahedral Ru(II) to two bidentate bipyridine ligands with two imidazole ligands or a water and an *N*-methylimidazole ligand cis to each other. The importance of these molecules is associated with their frequent use in the modification of proteins at histidine residues and in comparisons of the modified protein derivatives with these small molecule analogs.

Introduction

Tris(bipyridine)ruthenium(II), $[Ru(bpy)_3]^{2+}$, and bis(bipyridine)ruthenium(II) *cis*-$[Ru(bpy)_2L_2]^{2+}$ derivatives have been used as donors and acceptors in studies of long range intramolecular electron transfer in peptides and proteins.[1−4] Protein modification with functionalized tris(bipyridine)ruthenium(II) derivatives has resulted in the binding of these derivatives to lysine and cysteine residues.[2] Protein modification with *cis*-$[Ru(bpy)_2(OH_2)_2]$ and *cis*-$[Ru(bpy)_2(OH_2)L]$ results in proteins bound to the ruthenium center at the imidazole nitrogen of histidine residues.[1b,2a,3b]

Protein derivatives such as *cis*-$[Ru(bpy)_2L(protein)]$ (L = imidazole (Im)), where the protein is bound to the imidazole of the histidine residue, exhibit relatively long-lived excited states and a rich redox chemistry that have led to their use in the study of radiation-induced and photoinduced electron transfer reactions.[1b,2a,3b] Other bis(bipyridine)$Ru(L)_2$ complexes with L= pyridine derivatives show significantly lower quantum yields and shorter lifetimes at room temperature.[5]

In order to compare the properties of the ruthenium site in ruthenium modified proteins such as, *cis*-$[Ru(bpy)_2L(protein)]$ (L = Im) with small molecule analogues, we have studied the spectral, electrochemical, kinetic, and structural properties of a series of *cis*-$[Ru(bpy)_2(OH_2)L]$ (L = *N*-methylimidazole (N-Im)) and *cis*-$[Ru(bpy)_2L_2]$ (L = imidazole (Im)) ruthenium bipyridine complexes with one and two imidazole ligands, respectively. Some of the spectral and electrochemical properties for *cis*-$[Ru(bpy)_2L_2]$ (L = Im and N-Im) have been reported earlier, primarily in organic media.[6,7] In this work we report on the synthesis and properties of these complexes under conditions suitable for protein modification experiments.

Experimental Section

Materials. $RuCl_3$ was obtained from Matthey Bishop, and $Ru(bpy)_2Cl_2$ was obtained from Strem Chemical Co. All the chemicals used were reagent grade. Imidazole (Im) was recrystallized from water. The solvents were spectrophotometric grade and were used as is. The $Ru(bpy)_2Cl_2$ (bpy = 2,2′-bipyridine), $Ru(dmbpy)_2Cl_2$ (dmbpy = 4,4′-dimethyl-2,2′-bipyridine), $Ru(bpy)_2CO_3$ and $Ru(dmbpy)_2CO_3$ were prepared according to literature procedures.[8−10] C_{18} reverse phase silica gel resin (S-50) was purchased from YMC Co., Ltd.

***cis*-[Ru(bpy)$_2$(L)(H$_2$O)](CF$_3$COO)$_2$ [L = Im (imidazole), N-Im (*N*-methylimidazole)].** The $Ru(bpy)_2CO_3$ (100 mg, 0.22 mmol) was dissolved in 10 mL of deaerated water containing several drops of 1

† Present address: Department of Chemistry, Brookhaven National Laboratory, Upton, NY 11973.

⊗ Abstract published in *Advance ACS Abstracts,* November 1, 1996.

(1) See, for example: (a) Isied, S. S.; Ogawa, M. Y.; Wishart, J. F. *Chem. Rev.* **1992**, *92*, 381. (b) Isied, S. S. In *Electron Transfer in Biology and the Solid State, Inorganic Compounds with Unusual Properties;* Johnson, M. K., King., R. V., Kurtz, D. M., Jr., Kutal, G., Norton, M. L., Scott, R. A., Eds.; Advances in Chemistry 226; American Chemical Society: Washington, DC, 1990; pp 91−100.

(2) (a) Durham, B.; Pan, L. P.; Hahm, S.; Long, J.; Millett, F. In *Electron Transfer in Biology and the Solid State, Inorganic Compounds with Unusual Properties*; Johnson, M. K., King, R. V., Kurtz, D. M., Jr., Kutal, G., Norton, M. L., Scott, R. A., Eds.; Advances in Chemistry 226; American Chemical Society: Waashington, DC, 1990; pp 181−196. (b) Millet, F. In *Metal Ions in Biological Systems*; Sigel, H., Sigel, A., Eds.; Marcel Dekker: New York, 1991; pp 223. (c) Scott, J. R.; McLean, M.; Sligar, S. G.; Durham, B.; Millett, F. *J. Am. Chem. Soc.* **1994**, 116, 7356−7362. (d) Scott, J. R.; Willie, A.; McLean, M.; Stayton, R. S.; Sligar, S. G.; Durham, B.; Millett, F. *J. Am. Chem. Soc.* **1993**, *115*, 6820−6824. (e) Willie, A.; McLean, M.; Lieu, R.; Hilgen-Willis, S.; Aunders, A. J.; Pielak, G. J.; Sligar, S. G.; Durham, B.; Millett, F. *Biochemistry*, **1993**, *32*, 7519−7525. (f) Durham, B.; Pan., L.; Long, J.; Millett, F. *Biochemistry*, **1989**, *28*, 8659.

(3) (a) Langen, R.; Chang, I.; Germanas, J. P.; Richards, J. H.; Winkler, J. R.; Gray, H. B. *Science* **1995**, *268*, 1733. (b) Winkler, J. R.; Gray, H. B. *Chem. Rev.* **1992**, *92*, 369.

(4) (a) Schanze, K.; Sauer, K. *J. Am. Chem. Soc.* **1988**, 110, 1180. (b) Schanze, K.; Cabana, L. A. *J. Phys. Chem.* **1990**, *94*, 2740.

(5) Juris, A.; Balzani, V.; Barigelletti, S.; Campagna, S.; Belser, P.; Von Zelewsky, A. *Coord. Chem. Rev.* **1988**, *84*, 85.

(6) Sullivan, B. P.; Salmon, D. J.; Meyer, T. J. *Inorg. Chem.* **1978**, *17*, 3334.

(7) Long, C.; Vos, J. G. *Inorg. Chim. Acta* **1984**, *89*, 125.

(8) Johnson, E. C.; Sullivan, B. P.; Meyer, T. J. *Inorg. Chem.* **1978**, *17*, 2211.

(9) Marmion, M. E.; Takeuchi, K. J. *J. Am. Chem. Soc*. **1988**, *110*, 1472.

(10) Caspar, J. V.; Meyer, T. J. *Inorg. Chem*. **1983**, *23*, 2444.

S0020-1669(95)01434-0 CCC: $12.00

M trifluoroacetic acid (HTFA) and degassed with argon for 0.5 h. The pH of this cis-$[Ru(bpy)_2(H_2O)_2]^{2+}$ solution was adjusted to pH 11.5 by dropwise addition of degassed 1 M NaOH. To this solution 25 mg of L (0.37 mmol) was added and the reaction mixture was stirred under argon atmosphere for 2 h. The progress of the reaction was monitored with HPLC. At the end of the reaction the solution was concentrated to dryness by rotary evaporation. A few drops of 1 M HTFA were added slowly to the solid cis-$[Ru(bpy)_2(L)(OH)](TFA)$. When this mixture was cooled in an ice bath for about 2 h, a wine-red solid cis-$[Ru(bpy)_2(L)(H_2O)](TFA)_2$ precipitated. This solid was filtered and washed with several volumes of ether and dried thoroughly in a vacuum desiccator. The solid was redissolved in a minimum of water and purified on C-18 column (2.5 cm × 2.5 cm gravity column packed with C-18 resin (particle size ~50 μm)) by eluting with 5% ethanol in water. The purity of the final product was confirmed by electrochemistry and HPLC. Yields ranged from 60 to 70%. Crystals of *cis*-$[Ru(bpy)_2(N\text{-}Im)(H_2O)](CF_3COO)_2$ suitable for X-ray diffraction studies were obtained by slow evaporation of solvent from a concentrated solution of cis-$[Ru(bpy)_2(N\text{-}Im)(H_2O)]^{2+}$ in methanol.

***cis*-[Ru(dmbpy)(Im)(H$_2$O)](CF$_3$COO)$_2$.** The same procedure was used as described for the cis-$[Ru(bpy)_2(L)(H_2O)](TFA)_2$, except the pH of $[Ru(dmbpy)_2(H_2O)_2]^{2+}$ solution was adjusted to 11.0.

***cis*-[Ru(bpy)$_2$(L)$_2$]$^{2+}$ and *cis*-[Ru(dmbpy)$_2$(L)$_2$]$^{2+}$ (L = Im, N-Im).** These complexes were prepared according to literature procedures.[6a] Crystals suitable for X-ray diffraction were obtained by slow evaporation of methanol from a concentrated solution of *cis*-$[Ru(bpy)_2(Im)_2](BF_4)_2$.

Instruments and Techniques. HPLC of the complexes was carried out using a Waters μ-Bondapak C-18 reverse phase column. UV−vis spectra were recorded on a Hewlett Packard 8452A diode array spectrophotometer. Reduction potentials of complexes were determined by cyclic voltammetry using a three-electrode configuration (glassy carbon working electrode, SCE reference electrode, platinum auxillary electrode) with a BAS 100A instrument (Bioanalytical Systems, West Lafayette, IN).

Emission spectra were measured in 1-cm quartz cells using a Spex Industries Fluoromax spectrofluorimeter. The solutions used for emission studies were thoroughly degassed with argon. Emission quantum yields were determined at room temperature by comparing the emission of samples of known concentration to the emission of a standard sample of $[Ru(bpy)_3]^{2+}$ (ϕ_{em} = 0.089 in 4:1 EtOH/MeOH solution).[11,12] Luminescence decay measurements were performed with a PRA single photon counting system[13] using a PRA 510B lamp (6−8 kV, $^1/_2$ atm of H_2, 30−35 kHz flash rate, and 2−3 mm electrode spacing). The excitation wavelength was 470 nm, and the emission wavelengths were 610 or 670 nm. The emission was detected with a cooled Hamamatsu R929 photomultiplier. The first-order decay curves were fit using an iterative Levenberg−Marquardt fitting routine.

The rate of water substitution by imidazole in *cis*-$[Ru(bpy)_2(Im)(H_2O)]^{2+}$ was studied under pseudo-first-order conditions ([Im] ≫ [Ru(II)]) at 25 °C, pH 7.5, [Ru] = 7.0×10^{-5} M, and [Im] = 0.056−0.45 M. The reactions were monitored by recording the intensity changes at the emission maximum of the product as a function of time and the concentration of imidazole ligand using a Spex Fluoromax spectrofluorometer. The kinetics of aquation of imidazole from *cis*-$[Ru(bpy)_2(Im)_2]^{2+}$ were studied by monitoring the decrease in intensity of fluorescence at its maximum emission using initial rate methods.[14]

X-ray Crystallography. Single-crystal X-ray diffraction data were collected for crystals of *cis*-$[Ru(bpy)_2(N\text{-}Im)(H_2O)](CF_3COO)_2$ and *cis*-$[Ru(bpy)_2(Im)_2](BF_4)_2$ using a CAD4 diffractometer with graphite-monochromatized Mo Kα radiation (λ = 0.710 73 Å). For each data collection, the intensities of three standard reflections did not change significantly throughout the experiment. The data were corrected for Lorentz effects and polarization. On the basis of the ψ scans, absorption effects were minor, and no absorption corrections were made. The crystal structures were solved by Patterson methods (SHELXS 86).[15] All non-hydrogen atom positions and anisotropic displacement parameters were refined using full-matrix least-squares methods based upon F_o^2 (SHELXL93).[16] All hydrogen atom coordinates were calculated with bond distances of 0.95 Å. Crystallographic data for *cis*-$[Ru(bpy)_2(N\text{-}Im)(H_2O)](CF_3COO)_2$ and *cis*-$[Ru(bpy)_2(Im)_2](BF_4)_2$ are presented in Table 4. Selected bond distances and bond angles are given in Table 5. The atomic coordinates for the structures are given as Supporting Information.

Results and Discussion

Synthesis: The preparation of *cis*-$[Ru(bpy)_2L(H_2O)]^{2+}$, L = imidazole or pyridine ligands, reported here is based on the following reactions (eqs 1−3). In this sequence, the *cis*-$[Ru(bpy)_2(OH)(H_2O)]^+$, generated by the addition of base under inert atmosphere, undergoes substitution by only one ligand L (eq 2) to form *cis*-$[Ru(bpy)_2(OH)L]^+$. Rapid addition of CF_3COOH (eq 3) generates the cis-$[Ru(bpy)_2L(H_2O)]^{2+}$, which can be crystallized as a TFA salt. The same procedure was also used for the related *cis*-$[Ru(dmbpy)_2L(H_2O)]^{2+}$ complexes where L = *N*-methylimidazole (N-Im) and dmbpy = 4,4′-dimethyl-2,2′-bipyridine.

$$cis\text{-}[Ru(bpy)_2(H_2O)_2]^{2+} + OH^- \rightarrow cis\text{-}[Ru(bpy)_2(OH)(H_2O)]^+ + H_2O \quad (1)$$

$$cis\text{-}[Ru(bpy)_2(OH)(H_2O)]^+ + L \rightarrow cis\text{-}[Ru(bpy)_2(L)(OH)]^+ + H_2O \quad (2)$$

$$cis\text{-}[Ru(bpy)_2(L)(OH)]^+ + 2CF_3COOH \rightarrow cis\text{-}[Ru(bpy)_2(L)(H_2O)](CF_3COO)_2 + H^+ \quad (3)$$

The synthetic procedures described in this paper were developed for the purpose of using these ruthenium bipyridine complexes to modify electron transfer proteins.[1b] Earlier procedures for the preparation of cis-$[Ru(bpy)_2L(H_2O)]^{2+}$ complexes by the reaction of cis-$[Ru(bpy)_2LCl]^+$ with silver perchlorate in ethanol/water or acetone/water solution under reflux conditions[7,17,18] are not easily adaptable to the substitution of the resulting ruthenium complexes on proteins.

UV−vis Spectra and Electrochemistry: The absorption spectra of the *cis*-$[Ru(bpy)_2(N\text{-}Im)(H_2O)](CF_3COO)_2$ and cis-$[Ru(bpy)_2(Im)_2](BF_4)_2$ complexes are shown in Table 1. Also shown for comparison in Table 1 are the corresponding complexes where the bpy is replaced by dmbpy. Small changes in the metal-to-ligand charge transfer band (MLCT) (dπ(Ru)−π*(bpy)) are observed (ranging from 486 nm to 494 nm). All the complexes show bands at around λ = 340 nm (MLCT (dπ(Ru)−π_2*(bpy)) and bands at about λ = 240 and 290 nm ($\pi-\pi$* transitions of bipyridine ligands).

The cyclic voltammetric measurements in 0.1 M NaTFA (pH = 3.0) for the complexes are also reported in Table 1. All the complexes showed a reversible wave for the Ru(III)/Ru(II) redox couple ranging from 0.79 to 1.0 V vs NHE. The redox potentials for complexes with alkyl-substituted bipyridines were lower than the corresponding unsubstituted analogues because the electron-donating inductive effect of the methyl groups makes Ru(II) more electron rich, thus raising the energy of the

(11) Barqawi, K. R.; Murtaza, Z.; Meyer, T. J. *J. Phys. Chem.* **1991**, *95*, 47.
(12) Cook, M. J.; Thompson, A. J. *Chem. Br.* **1984**, 914.
(13) Synder, S. W.; Demas, J. N.; deGraff, B. A. *Anal. Chem.* **1989,** *16*, 2704.
(14) Espenson, J. H. *Chemical Kinetics and Reaction Mechanisms*; McGraw-Hill: New York, 1981.
(15) Sheldrick, G. M. SHELX 86, Program for the Solution of Crystal Stucture. University of Gottingen, Germany, 1986.
(16) Sheldrick, G. M. SHELX 93, Program for Crystal Structure Refinement. University of Gottingen, Germany, 1993.
(17) Marmion, M. E.; Takeuchi, K. J. *J. Am. Chem. Soc.* **1988**, *110*, 1472.
(18) Kalsbeck, W. A.; Thorp, H. H. *Inorg. Chem.* **1994**, *33*, 3427.

Table 1. UV−Vis Spectroscopic and Electrochemical Data for *cis*-Bis(bipyridine)ruthenium(II) Complexes

complex	λ_{max}, nm ($\epsilon \times 10^{-4}$, M^{-1} cm^{-1})				$E_{1/2}$[a] (V vs NHE)
$[Ru(bpy)_2(Im)(H_2O)]^{2+}$	242 (2.93)	290 (7.50)	340 (0.963)	486 (1.21)	0.85
$[Ru(bpy)_2(N\text{-}Im)(H_2O)]^{2+}$	242 (2.77)	290 (6.77)	340 (0.900)	486 (1.14)	0.83
$[Ru(bpy)_2(Im)_2]^{2+}$	242 (1.91)	292 (4.71)	340 (0.660)	490 (0.746)	1.00
$[Ru(dmbpy)_2(Im)(H_2O)]^{2+}$	248[b]	290	336	490	0.79
$[Ru(bpy)_2(N\text{-}Im)_2]^{2+}$	244[b]	292	340	490	1.01
$[(Ru)(dmbpy)_2(Im)_2\}^{2+}$	246[b]	290	338	492	0.87
$[Ru(dmbpy)_2(N\text{-}Im)_2]^{2+}$	248[b]	290	340	494	0.87

[a] 0.1 M NaTFA (pH = 3). [b] References 6, 7, and 23.

Table 2. Emission Properties of *cis*-Bis(bipyridine)ruthenium(II) Complexes[a]

complex	λ_{em}, nm	$\Phi_{em} \times 10^4$	τ, ns
$[Ru(bpy)_2(Im)_2]^{2+}$	662	26.0	61.0
$[Ru(dmbpy)_2(Im)_2]^{2+}$	666	20.0	42.0
$[Ru(bpy)_2(N\text{-}Im)_2]^{2+}$	662	30.0	70.0
$[Ru(dmbpy)_2(N\text{-}Im)_2]^{2+}$	666	26.0	47.0
$[Ru(bpy)_2(Im)(H_2O)]^{2+}$	(665)[b]	≤0.550[b]	c
$[Ru(bpy)_2(N\text{-}Im)(H_2O)]^{2+}$	(666)[b]	≤0.700[b]	c
$[Ru(bpy)_3]^{2+}$	603[d]	420[d]	580[d]

[a] In 50 mM phosphate buffer (pH = 7.0) at room temperature. [b] The quantum yield was determined as the lower limit from the fluorescence spectra. This low emission quantum yield may also result from the presence of 1−2% $[Ru(bpy)_2(Im)_2]^{2+}$ or $[Ru(bpy)_2(N\text{-}Im)(H_2O)]^{2+}$ which was undetectable in the HPLC or DPP at pH 7. [c] The lifetime was nondetectable (≤10 ns) with the experimental setup used. [d] In aqueous solution.

highest occupied molecular orbital and reducing the Ru(II) capacity for π-back-donation.

Emission Spectra. The emission properties of *cis*-$[Ru(bpy)_2(N\text{-}Im)(H_2O)]^{2+}$, *cis*-$[Ru(bpy)_2(Im)_2]^{2+}$ and related complexes at 25°C are summarized in Table 2. Very small differences are observed between the emission maxima of the ruthenium complexes. However major differences are found among the emission quantum yields and lifetimes of the excited states. As seen in Table 2, the presence of a H_2O ligand reduces the emission quantum yield by at least two orders of magnitude and decreases the lifetime significantly (ca. <10 ns).[25] The emission lifetimes of the *cis*-$[Ru(bpy)_2(Im)_2]^{2+}$ and other bis(imidazole) derivatives is reduced from 70 ns for cis-$[Ru(bpy)_2(N\text{-}Im)_2]^{2+}$ to 42 ns for *cis*-$[Ru(dmbpy)_2(Im)_2]^{2+}$. This correlates with a trend in the $E_{1/2}$ of the corresponding Ru(II/III) complexes. The lifetimes of the complexes were determined in phosphate buffer at pH 7 to enable comparison with the corresponding ruthenium-modified proteins under similar conditions.

Rates and Equilibria for the Substitution of Imidazole on *cis*-$[Ru(bpy)_2(Im)(H_2O)]^{2+}$. The difference in fluorescence intensity between the reactant and product in eq 4 provides a convenient method for monitoring the formation and hydrolysis of imidazole in this reaction. The rate was studied at total imidazole concentrations ranging from 0.056 to 0.45 M at pH 7.5. At pH 7.5, the effective imidazole concentration (after correction for the protonation of imidazole, pK 7.17[24]) ranged

$$cis\text{-}[Ru(bpy)_2(Im)(H_2O)]^{2+} + Im \underset{k_{-4}}{\overset{k_4}{\rightleftharpoons}} cis\text{-}[Ru(bpy)_2(Im)_2]^{2+} + H_2O \quad (4)$$

from 0.018 to 0.14 M. The plot of k_{obs} vs imidazole concentration was found to be linear with an intercept near zero (within experimental error). The rate of substitution k_4 was found to be $(7.0 \pm 1.0) \times 10^{-4}$ M^{-1} s^{-1} at 25 °C for an ionic strength of 0.03−0.3 M. The aquation rate constant (k_{-4}), determined by measuring the decrease in fluorescence intensity of *cis*-$[Ru(bpy)_2(Im)_2]^{2+}$ (in the absence of light) is $(2.5 \pm 0.5) \times 10^{-6}$ s^{-1}. From these two rate constants, the affinity of this ruthenium(II) complex for imidazole is $K_4 = 3 \pm 1 \times 10^2$ M^{-1}. These studies were carried out at pH 7.5 where there is negligible interference from the deprotonation of the imidazole ligands (the pK_a of the first and second imidazoles in *cis*-$[Ru(bpy)_2(Im)_2]^{2+}$ are 11.9 and 13.3 while that of the excited state is 10.8).[7] The substitution rate constant determined for imidazole here is similar to the rates observed for related nitrogenous ligands on ruthenium polypyridine complexes (Table 3).[22,23] In *cis*-$[Ru(bpy)_2(Im)(H_2O)]^{2+}$ the rate of substitution of water by nitrogenous ligands is more than 2 orders of magnitude slower than the rate of substitution on similar $[Ru(NH_3)_5(H_2O)]^{2+}$ complexes. Furthermore, the affinity of imidazole (Im) to *cis*-$[Ru(bpy)_2(Im)(H_2O)]^{2+}$ (K = 300 M^{-1}) is more than 4 orders of magnitude smaller than the affinity of imidazole to $[Ru(NH_3)_5(H_2O)]^{2+}$ ($K \sim 2.8 \times 10^6$ M^{-1}).[24] A similar study with L = pyrazine (pz), a much weaker base than imidazole, showed that its affinity to *cis*-$[Ru(bpy)_2(pz)(OH_2)]$ is only $K \sim 20$ M^{-1}, whereas the affinity of $[Ru(NH_3)_5(H_2O)]^{2+}$ for pyrazine is $K > 10^9$ M^{-1}.[22]

The rates and equilibria of the ruthenium(II) complexes for imidazole ligands are important in understanding the time course of protein modification of *cis*-$[Ru(bpy)_2(Im)(H_2O)]^{2+}$ on histidine residues and the residence time of the resulting modified protein species. Further studies on these model complexes in comparison to the modified proteins may elucidate the role that the proteins play in modifying the properties of these bound ruthenium complexes.

The comparison between the *cis*-$[Ru(bpy)_2L(OH_2)]$ and the corresponding *cis*-$[Ru(NH_3)_4L(OH_2)]$ complexes clearly shows a substantial decrease in the rates of substitution of the bipyridine series (Table 3) and also a decrease in the affinity for monodentate ligands.[21,22]

Crystal Structure. The crystal structures of *cis*-$[Ru(bpy)_2(N\text{-}Im)(H_2O)](CF_3COO)_2$ and *cis*-$[Ru(bpy)_2(Im)_2](BF_4)_2$ are shown in Figures 1 and 2, respectively, and the relevant crystallographic data and bond distances and angles are given in Tables 4 and 5.

The structure of *cis*-$[Ru(bpy)_2(N\text{-}Im)(H_2O)](CF_3COO)_2 \cdot H_2O$ (Figure 1a) consists of an octahedral Ru(II) coordinated to two bidentate bipyridine ligands with a water molecule and a N-Im ligand that are *cis* to each other. The Ru−N distances for the bipyridine ligands are 2.04−2.05 Å, the Ru−N(imidazole)

(19) Eggelston, D. S.; Goldsby, K. A.; Hodgson, D. J.; Meyer, T. J. *Inorg. Chem.* **1985**, *24*, 4573.
(20) Heeg, M. J.; Kroener, R.; Deutsch, E. *Acta Crystallogr.* **1985**, *C41*, 684.
(21) Isied, S. S.; Taube, H. *Inorg. Chem.* **1976**, *15*, 3070.
(22) Davies, N. R.; Mullins, T. L. *Aust. J. Chem.* **1968**, *21*, 915.
(23) Allen, N. R.; Craft, P. P.; Durham, B.; Walsh, J. *Inorg. Chem.* **1987**, *26*, 53.
(24) Sundberg, R. J.; Martin, R. B. *Chem. Rev.* **1974**, *74*, 471.
(25) The low emission quantum yield and lifetime of the aquo complexes is presumably related to the presence of a d−d state of similar energy to the MLCT state and/or the dissipation of energy of the excited state to solvent by H-bonding of solvent water to coordinated water.

Table 3. Substitution Rates for Imidazole and Related Ligands on Ruthenium(II) Bipyridine and Ammine Complexes[a]

$$[Ru(N)_4(X)(H_2O)]^{2+} + L \rightarrow [Ru(N)_4(X)(L)]^{2+} + H_2O$$

complex	L	k (L mol^{-1} s^{-1})	ref
$[Ru(bpy)_2(Im)(H_2O)]^{2+}$	Im	2.0×10^{-4}	this work
$[Ru(bpy)_2(H_2O)_2]^{2+}$	py	1.1×10^{-3}	22
$[Ru(bpy)_2(H_2O)_2]^{2+}$	CH_3CN	80×10^{-3}	23
$[Ru(bpy)(terpy)(H_2O)]^{2+}$	py	9.16×10^{-5}	22
$[Ru(bpy)_2(py)(H_2O)]^{2+}$	CH_3CN	10×10^{-5}	23
$[Ru(terpy)(bpy)(H_2O)]^{2+}$	isn	7.0×10^{-5}	21
$[Ru(terpy)(en)(H_2O)]^{2+}$	isn	3.0×10^{-2}	21
$[Ru(NH_3)_4(Im)(H_2O)]^{2+}$	isn	1.0×10^{-1}	21
$[Ru(NH_3)_4(py)(H_2O)]^{2+}$	isn	0.7×10^{-1}	21

[a] Im = imidazole; isn = isonicotinamide; terpy = 2,2′,2″-terpyridine; en = ethylenediamine; CH_3CN = acetonitrile; py = pyridine.

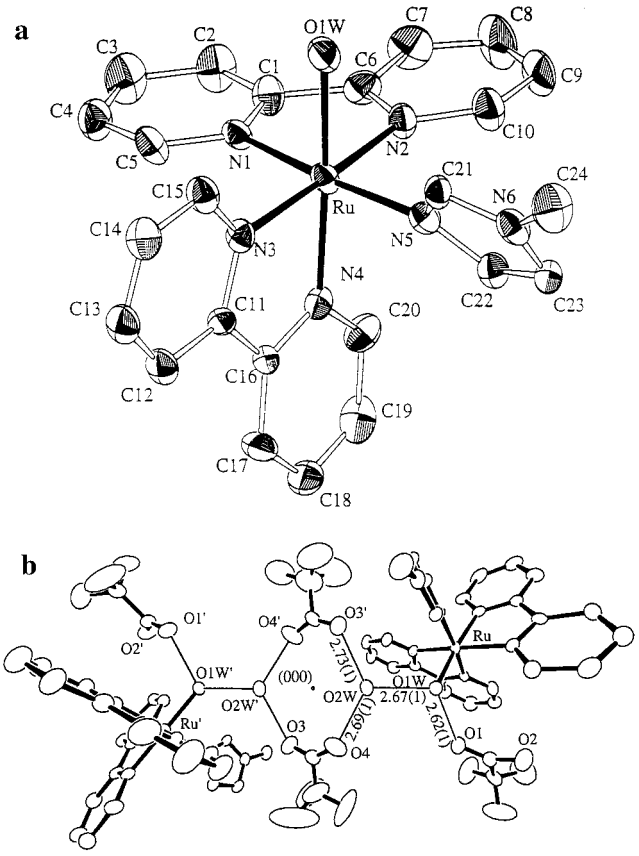

Figure 1. (a) ORTEP diagram and atom labeling scheme for *cis*-[Ru(bpy)$_2$(N-Im)(H$_2$O)](CF$_3$COO)$_2$·H$_2$O. Ellipsoids are drawn at the 30% probability level. The H atoms, water solvent molecule and counter ions are omitted for clarity. (b) ORTEP diagram showing *cis*-[Ru(bpy)$_2$(N-Im)(H$_2$O)](CF$_3$COO)$_2$·H$_2$O including the solvent water and trifluoroacetate counter ions.

distance is 2.08 Å, and the Ru−O bond distance is 2.13 Å. These distances are in good agreement with values reported for similar complexes.[19,20] The dihedral angles between the planes of the bipyridine and N-Im ligands are 87° (bpy#1−bpy#2), 58° (bpy#1−N-Im) and 87° (bpy#2−N-Im). There is one water molecule of solvation per ruthenium complex, resulting in a formula of [Ru(bpy)$_2$(N-Im)(H$_2$O)](CF$_3$COO)$_2$·H$_2$O.

The water of solvation is important for the hydrogen bonding network in the crystal packing motif. The hydrogen bonding scheme is shown in Figure 1b. The ligand water molecule is hydrogen bonded to one trifluoroacetate ion (O−O distance 2.62 Å) and the water of crystallization connects one ruthenium complex to its enantiomer across a symmetric hydrogen-bonding

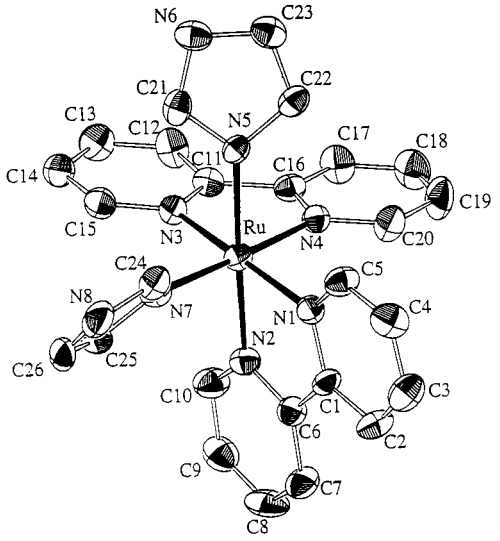

Figure 2. ORTEP diagram and atom labeling scheme for *cis*-[Ru(bpy)$_2$(Im)$_2$](BF$_4$)$_2$. Ellipsoids are drawn at the 30% probability level. The H atoms and counterions are omitted for clarity.

Table 4. Crystallographic Data for *cis*-[Ru(bpy)$_2$(N-Im)(H$_2$O)](CF$_3$COO)$_2$ and *cis*-[Ru(bpy)$_2$(Im)$_2$](BF$_4$)$_2$

	[Ru(bpy)$_2$(N-Im)(H$_2$O)](CF$_3$COO)$_2$	[Ru(bpy)$_2$(Im)$_2$](BF$_4$)$_2$
empirical formula	$C_{28}H_{26}F_6N_6O_6Ru$	$C_{26}H_{22}B_2F_8N_8Ru$
fw	757.62	721.21
a, Å	10.432(4)	11.344(1)
b, Å	11.995(3)	17.499(3)
c, Å	13.912(5)	15.114(3)
α, deg	87.03(3)	90.00(1)
β, deg	70.28(3)	100.17(1)
γ, deg	71.57(2)	90.00(1)
V, Å^3	1551.8(9)	2953.1(8)
Z	2	4
cryst syst	triclinic	monoclinic
space group	$P\bar{1}$	$P2_1/a$
scan mode	ω:θ	ω
ρ(calcd), g cm^{-3}	1.621	1.622
cryst dimens, mm	0.21 × 0.08 × 0.02	0.18 × 0.14 × 0.04
T, K	293 (2)	293 (2)
λ,[b] Å	0.71073 (Mo Kα)	0.710 73 (Mo Kα)
abs coeff, mm^{-1}	0.593	0.614
θ range, deg	2−22	2−22
tot. no. of reflcns measd	4305	3805
obsd [I>2σ(I)]	2504	2062
R_F [I>2σ(I)][a]	0.072	0.047
R_{wF} [I>2σ(I)][a]	0.176	0.084
GOF[a]	1.017	1.008
residuals, e Å^{-3}	+0.91 to −0.73	+0.46 to −0.44

[a] $R_F = \sum||F_o| - |F_c||/\sum|F_o|$; $R_{wF} = \{\sum w(F_o^2 - F_c^2)/\sum[w(F_o^2)]\}^{1/2}$; GOF = $[\sum w(F_o^2 - F_c^2)/(N_{obs} - N_{parm})]^{1/2}$. [b] Graphite monochromatized.

network centered on the inversion center at the origin of the unit cell. Two trifluoroacetate ions, related by inversion, form the "arms" of a chair-shaped, eight-atom ring with the included waters at the ends (O−O distances 2.69 and 2.73 Å) to complete the network (Figure 1b).

The F atoms in CF_3 show considerable disorder (i.e. large thermal parameters) as is common for CF_3 structures. The final refinement cycles for the *cis*-[Ru(bpy)$_2$(N-Im)(H$_2$O)](CF$_3$COO)$_2$ structure included restraints for all the C−F bond distances (1.32 Å) and the C−C bond of the anion (1.50 Å), and intramolecular nonbonded C···F and F···F distances (2.37 and 2.10 Å, respectively). In the difference-Fourier map the maximum residuals are located close to the heavy Ru atom (0.9e/Å^3), and only moderate residuals (0.5 e/Å^3 or less) are near the two disordered CF_3 sites. For the H atom refinement, the isotropic

Table 5. Selected Bond Lengths (Å) and Angles (deg) for *cis*-$[Ru(bpy)_2(N\text{-}Im)(H_2O)](CF_3COO)_2 \cdot H_2O$ and *cis*-$[Ru(bpy)_2(Im)_2](BF_4)_2$

	$[Ru(bpy)_2(N\text{-}Im)(H_2O)](TFA)_2$		
Ru−N (4)	2.036 (10)	Ru−N (3)	2.043 (9)
Ru−N (1)	2.040 (9)	Ru−N (5)	2.081 (9)
Ru−N (2)	2.051 (9)	Ru−O (1W)	2.131 (10)
N(4)−Ru−N(1)	90.4 (4)	N(2)−Ru−N(5)	95.7 (4)
N(4)−Ru−N(2)	99.3 (4)	N(3)−Ru−N(5)	88.7 (3)
N(1) -Ru−N (2)	78.3 (4)	N(4)−Ru−O(1W)	171.6 (4)
N(4)−Ru−N(3)	79.1 (4)	N(1)−Ru−O(1W)	93.1 (4)
N(1)−Ru−N(3)	97.2 (4)	N(2)−Ru−O(1W)	88.9 (4)
N(2)−Ru−N(3)	175.3 (4)	N(3)−Ru−O(1W)	92.8 (4)
N(4)−Ru−N(5)	90.3 (4)	N(5)−Ru−O(1W)	87.1 (4)
N(1)−Ru−N(5)	174.0 (3)		
	cis-$[Ru(bpy)_2(Im)_2](BF_4)_2$		
Ru−N(2)	2.037(6)	Ru−N(3)	2.050(6)
Ru−N(4)	2.042(7)	Ru−N(5)	2.093(6)
Ru−N(1)	2.047(6)	Ru−N(7)	2.096(7)
N(2)−Ru−N(4)	89.3(3)	N(1)−Ru−N(5)	98.6(3)
N(2)−Ru−N(1)	78.9(3)	N(3)−Ru−N(5)	86.8(2)
N(4)−Ru−N(1)	96.4(3)	N(2)−Ru−N(7)	91.3(3)
N(2)−Ru−N(3)	95.7(3)	N(4)−Ru−N(7)	177.4(3)
N(4)−Ru−N(5)	79.1(3)	N(1)−Ru−N(7)	86.2(3)
N(1)−Ru−N(3)	173.1(3)	N(3)−Ru−N(7)	98.4(3)
N(2)−Ru−N(5)	177.3(3)	N(5)−Ru−N(7)	89.6(3)
N(4)−Ru−N(5)	90.0(3)		

displacement parameters (U_{iso}) were restrained to be equal for all the H atoms of one type; for phenyl group H atoms $U_{iso} = 0.7$ Å^2, for all methyl group H atoms $U_{iso} = 0.101$ Å^2, and for all the water molecule H atoms $U_{iso} = 0.086$ Å^2.

The *cis*-$[Ru(bpy)_2(Im)_2](BF_4)_2$ structure is a monomeric octahedral Ru(II) with two bidentate bpy ligands, and two imidazole ligands that are *cis* to one another. All the Ru-N distances (2.04−2.05 Å for the bpy ligands; 2.09−2.10 Å for the Im ligands) are as expected.[19,20] The dihedral angles between the calculated ligand planes are 85° (bpy#1−bpy#2), 53° (bpy#1−Im#1), 83° (bpy#1−Im#2), 84° (bpy#2−Im#1), 50° (bpy#2−Im#2), and 67° (Im#1−Im#2). In $[Ru(bpy)_2(Im)_2](BF_4)_2$ the crystal packing does not involve hydrogen bonding to the BF_4 anions. The two anions are disordered, and were modeled with 2-fold disorder to a moderate refinement. The final refinement cycles for the $[Ru(bpy)_2(Im)_2](BF_4)_2$ crystal structure included restraints for all the B−F bond distances (1.370 Å) and F···F (2.237 Å) intramolecular distances. The isotropic displacement parameters for the phenyl group H atoms ($U_{iso} = 0.058$ Å^2) were refined and restrained to be equal.

Acknowledgment. This research was supported by the U.S. Department of Energy, Division of Chemical Sciences, Office of Basic Energy Sciences under Contracts DE-FG05-90ER1410 and DE-FG02-93ER14356, and by the Center for Advanced Food Technology (CAFT) at Rutgers University.

Supporting Information Available: Tables of crystallographic data and refinement results, atomic coordinates, bond lengths and angles, anisotropic displacement parameters, hydrogen atom parameters, torsion angles, and figures showing projections of the unit cell packing (18 pages). Ordering and Internet access information is given on any current masthead pages. Structure factor listings are available from the authors.

IC951434B